

THE EFFECT OF BULB FREQUENCY ON THE  
BEHAVIOUR OF FULLY GROUTED GARFORD BULB  
CABLE BOLTS.

*By:*

A.J. HYETT

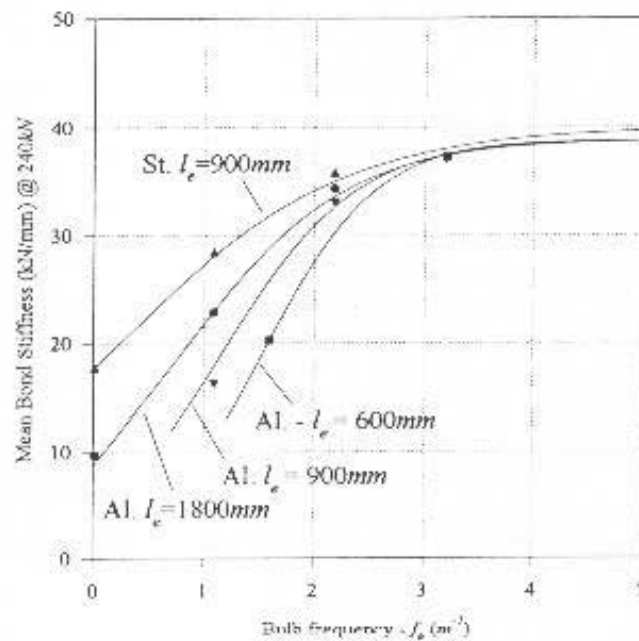
W.F. BAWDEN

*Department of Mining Engineering,  
Queen's University,  
Kingston,  
Ontario.  
K7L 3N6*

MARCH 1996

### EXECUTIVE SUMMARY

The results for 75 pull tests demonstrate the increased bond strength and bond stiffness of fully grouted Garford bulb cable compared to plain strand (see over). Furthermore, the stiffness of fully grouted Garford bulb cable can be controlled by varying the bulb frequency as shown below.

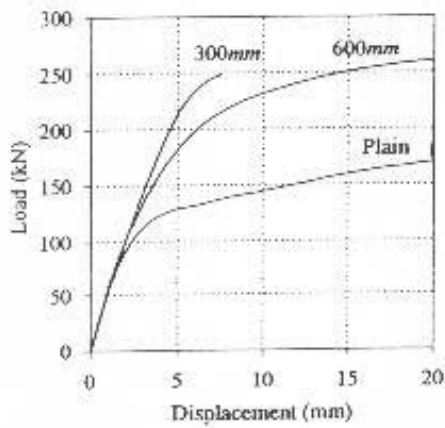


Mean bond stiffness ( $kN/mm$ ) versus bulb spacing.

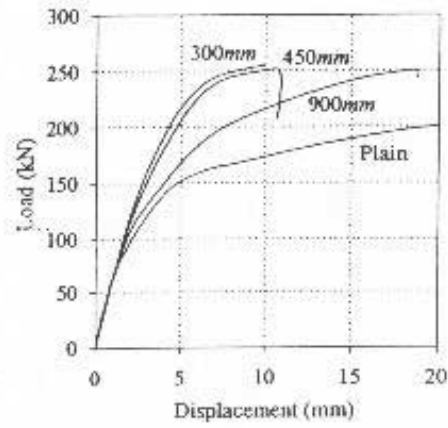
The test results indicate that for loads less than  $60kN$ , the bond stiffness was relatively independent of test parameters. However, at higher loads, the rate of load increase during a cable pull test (*i.e.* the stiffness of the grouted cable bolt) was higher for:

- (i) closer bulb spacings,
- (ii) longer embedment lengths, and,
- (iii) higher radial stiffness of the confining medium.

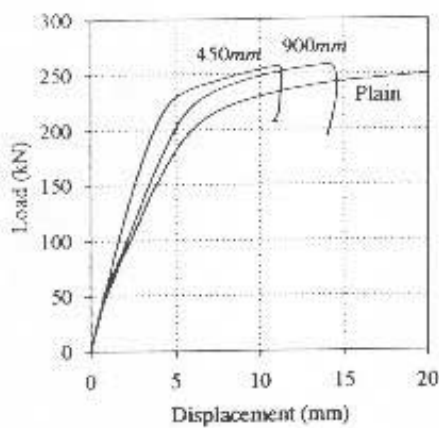
600mm E.L. Al-80 pipe



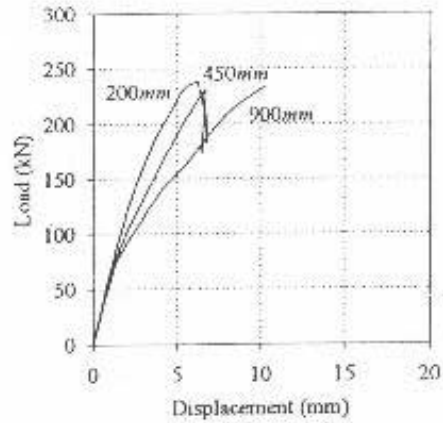
900mm E.L. Al-80 pipe



900mm E.L. St-80 pipe



1800mm E.L. Al-80 pipe



Summary of the pull test results. The Bulb spacing is indicated.

A combination of two effects can explain the results: for a closer bulb spacing:

- (i) the proportion of the cable comprised of plain cable which has a lower bond strength (and stiffness) is reduced, and
- (ii) the distance between the exit point and the first bulb is reduced, and hence that first bulb acts sooner during a test.

However, the authors believe as shown in the figure above, that there is a limit to how close together the bulbs should be positioned. For a 200mm bulb spacing there is very little plain cable between bulbs. Results indicate, that this may instigate a change in the mechanics of bond failure.

For bulb frequencies higher than  $3m^{-1}$  (i.e. bulb spacings greater than approx. 12"), 6mm of exit point displacement was required to mobilize 240kN, resulting in an average stiffness of 40kN/mm. For bulb frequencies lower than  $3m^{-1}$  (i.e. bulb spacings less than approx. 12"), in addition to bulb spacing, the stiffness was dependent on both the embedment length and the radial stiffness of the confining medium.

These results suggest that the Garford bulb requires a definite amount of relative slip with the cement in order to mobilize bond strength. This implies that *there is an upper limit to the bond stiffness of a Garford bulb cable bolt*. Comparable tests indicate that this stiffness is similar to that of a cement grouted 1" rebar.

#### *Implication for the design of point anchored bolts*

The concept of *transfer length* ( $l_t$ ) is widely used in civil engineering, especially applications in which pre-tension or post-tension is applied to the strand. Transfer length is defined as : *the length of bond required to transmit the applied tensile load from the member to the grout*. It is the distance along the bonded section at which the tensile stress in the member is less than a specified value (usually 1% of the applied axial load). Farmer(1975) suggests that "the transfer length is equivalent to the optimum design length for the fixed anchorage". For the application of point anchored strand bolts we introduce the concept of a **critical transfer length** defined as *that length of bond which ensures that when the ultimate capacity of the bolt is reached, no significant movement of the bolt has occurred at the toe of the bolt*. It is important to distinguish between critical transfer length and the **critical embedment length** defined as *the minimum length of bond necessary to ensure that the ultimate capacity of the bolt is attained*. The latter does not specify how much bond slip is allowed.

Based on the test results in this paper, for point anchored applications, for Garford bulb spacings greater than 300mm we recommend the relation:

$$\text{Critical Transfer Length} = 2 \times \text{Garford Bulb Spacing} \times \text{FOS}$$

## 1. Glossary of Terms.

### *Embedment Length ( $l_e$ ):*

The length of cable that is fully grouted.

### *Entry Point:*

That end of the specimen at which the cable enters the grout column during a pull test. *i.e.* the free end.

### *Exit Point:*

That end of the cable for which the cable exits the grout column during a pull test. *i.e.* the end at which load is applied.

### *Cable Capacity $F_c$ (kN):*

The axial force required to rupture the cable (approx. 260kN for 0.6" strand).

### *Cable Yield:*

Capacity at which the load-deformation behaviour indicates a departure from linear elasticity. (approx. 220-240kN)

### *Pullout Force $F_o$ (kN):*

The force applied at the exit point during pullout.

### *Cable Stiffness $K_c$ (kN/mm):*

The relation between force and displacement as the cable stretches, given by:

$$K_c = \frac{E_c A}{l}$$

where  $E_c$  is the axial modulus of the cable and  $A$  is the nominal cross-sectional area. Often quoted per/unit length in which case the units become: *kN/mm/mm*

### *Bond Slip $u_o$ (mm):*

The relative displacement between the cable and the grout occurring at the cable-grout interface.

### *Bond Stress $\tau$ (MPa):*

The corresponding shear stress mobilized at the cable-grout interface during pullout. For a specified embedment length ( $l_e$ ), knowing the force required for pull out ( $F_o$ ), the bond strength can be calculated as:

$$\tau = \frac{F_o}{A} = \frac{F_o}{2\pi r l_e}$$

where  $r$  is the radius of the bolt.

*Cable-Grout Bond Stiffness or just Bond Stiffness  $K_b$  (kN/mm):*

The slope of the relation between pull out force and slip at the exit point.

$$K = \frac{F_0}{u_0}$$

*Critical Embedment Length  $l_{ca}$  (m):*

The minimum embedment length for which the cable capacity can be mobilized during a pull test.

*Critical Transfer Length  $l_{ct}$  (m):*

The minimum embedment length for which, when the cable capacity can be mobilized during a pull test, there is no significant movement at the entry point.

*Radial Stiffness  $K_r$  (MPa/mm):*

The slope of the relation between radial pressure and radial deformation for the confining medium.

*Transfer Length  $l_t$  (m):* The length of fully grouted cable required to transmit the applied force to the grout.

*Bulb Spacing  $l_b$  (m)*

The distance from one Garford bulb to the next.

*Bulb Frequency  $f$  (m<sup>-1</sup>):*

$$f = 1/l_b$$

## 2. Introduction

Previous research (Fuller and Cox, 1975; Stilborg, 1984; Goris, 1990; Hyett *et al.*, 1992, Kaiser *et al.*, 1992) has established that for short bond lengths (typically 250mm), the pull out force for conventional 7-wire strand varies as a function of the grout properties, the rock mass properties and mining induced stress changes.

Hyett *et al.* (1995) conducted pull tests with a single 25mm Garford Bulb grouted midpoint along a 300mm embedment length. Loads close to, or in excess of, the ultimate capacity of the cable were attained under a variety of different radial confinements and grout qualities. This established that the effect of the bulb structure was to significantly increase resistance to pullout and the corresponding bond strength.

During the Garford Bulb manufacturing process it is possible to vary the spacing between bulbs. Hedrick (1995) proposed the bond stiffness during pullout will increase as the spacing between bulbs is reduced. With the exception of a small number of twin strand pull tests conducted by Strata Control (Garford, 1990) using embedment lengths up to 500mm (aprox 20"), no quantitative data suitable for engineering is available on this effect. This report describes a comprehensive test programme to investigate the effect of bulb spacing on the bond stiffness of Garford bulb cables. The data generated will provide a rational basis for the design of cable bolt patterns with different bulb spacings.

## 3. Laboratory Test Procedure.

The principal test parameters to be investigated were:

- (i) Garford bulb spacing (200mm, 300mm, 450mm, 900mm, plain)\*;
- (ii) (ii) embedment length (600mm, 900mm and 1800mm);
- (iii) (iii) radial stiffness of the confining medium (Sch. 80 steel pipe, Sch. 80 Aluminum pipe);

resulting in a test matrix comprising 75 tests (Table 1). The ranges selected for each parameter were based on the results from a preliminary test programme. Figure 1 shows the configuration of the bulbs along the test samples for each of the test series.

\*Since the test program was being conducted in N. America where the mining industry still uses Imperial units the bulb spacing and embedment lengths were actually specified in inches. To round of the corresponding metric values, and so improve readability, a conversion factor of 1"=25mm has been used throughout this report

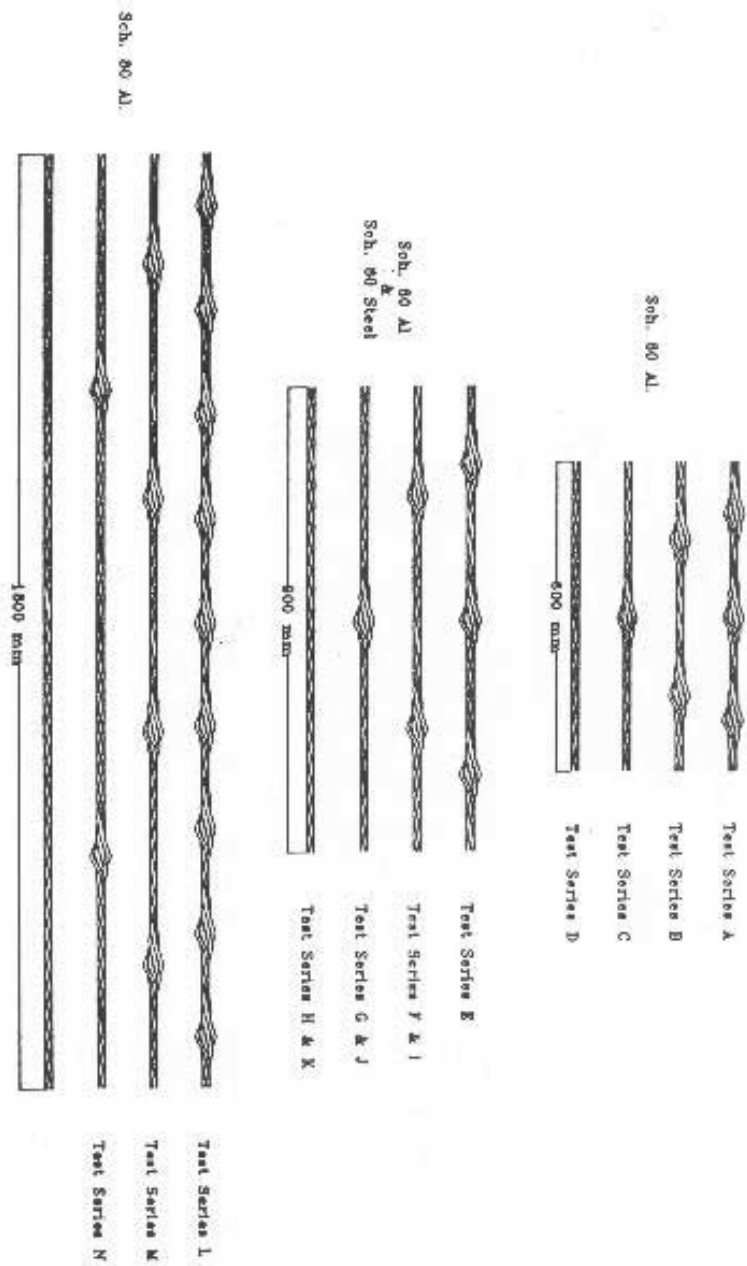


Figure 1: The bulb configuration for the different test series.

Test Series	Bulb Spacing ( $l_b$ ) (mm)						Confinement		Embedment length (mm)		
	200	300	450	600	900	$\infty$	AJ	Steel	600	900	1800
A	x						x		x		
B		x					x		x		
C				x			x		x		
D						x	x		x		
E		x					x			x	
F			x				x			x	
G					x		x			x	
H						x	x			x	
I			x					x		x	
J					x			x		x	
K						x		x		x	
L	x						x				x
M			x				x				x
N					x		x				x
O						x	x				x

Table 1. The pull test programme matrix.

It should be pointed out that two potentially important parameters have been ignored:

- (i) the grout w:c ratio (0.4 w:c for all tests).
  - mining operations familiar with cable bolting should be able to routinely pump a 0.4 w:c ratio grout which is regarded as providing an optimal trade-off between pumpability/flowability and strength.
- (ii) the distance between the exit point and the first bulb;
  - If a cable bolt with Garford bulbs spaced  $l_b$  apart was randomly located in a borehole, the location of the first bulb might lie anywhere between the end of the hole and a distance  $l_b$  away: the mean of this distance being  $l_b/2$ . Therefore, in this test programme bulbs were symmetrically located along the embedment length, with the extreme bulbs located at  $l_b/2$  from the exit point and the entry point.

For those test series with 600mm and 900mm embedment length, the setup shown in Figure 2 was used. For the 1800mm tests the sample was too long for the MTS machine, and the setup shown in Figure 3 had to be used. Since the objective of the experiments was to determine the stiffness of the grouted cable bolt, the displacement (*i.e.* slip) of the cable at both the exit point and the entry point were accurately measured.

In case the cable should break prematurely, the LVDT at the entry point was removed from the sample when the pullout load exceeded 200kN.

The samples were grouted using a 0.4 w:c ratio grout (specific gravity = 1.95), and pull testing commenced 26 days later.

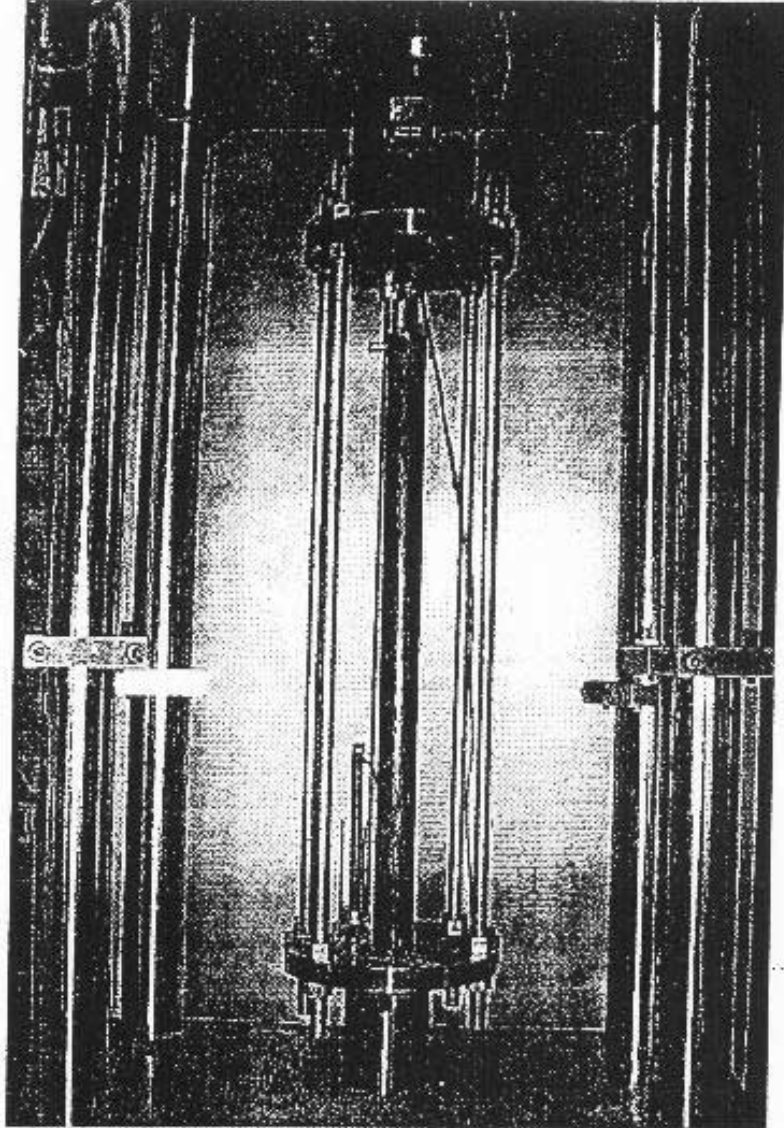
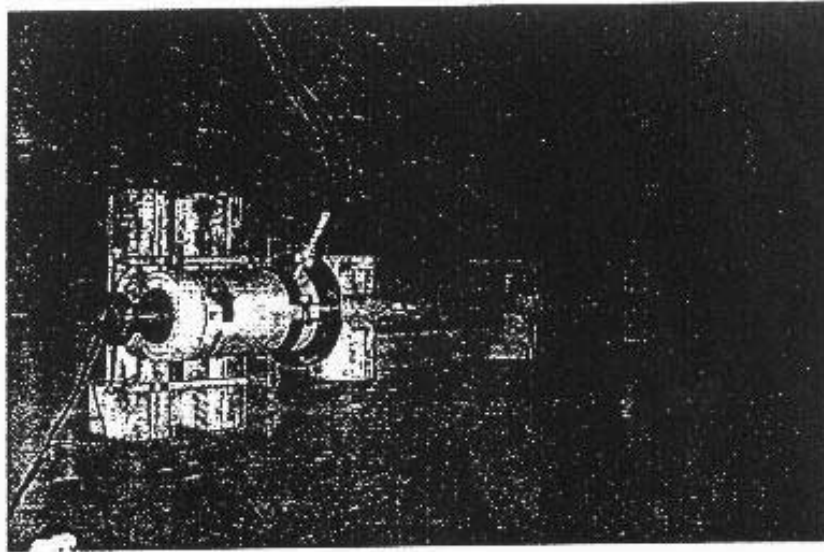
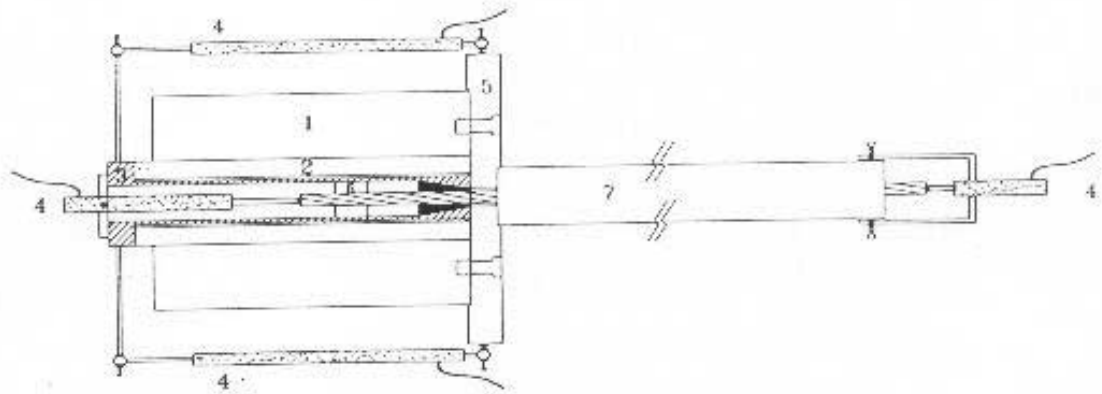


**Figure 2.** The pull test procedure in the MTS machine.



(a)



- 1. Hollow Ram Jack
- 2. Ram
- 3. Pulling pipe.
- 4. LVDTs.

- 5. Bearing plate.
- 6. Centralizer
- 7. Specimen.

(b)

Figure 3. The Long pipe test setup for embedment lengths longer than 900mm. LVDT #1 is at the exit point and LVDT #2 is at the entry point.

#### 4. Pull test results

The detailed pull test results are shown in Appendix A. The upper plot shows axial load ( $kN$ ) versus axial displacement at the exit point (mm); the lower plot entry point displacement (LVDT 2 - mm) versus exit point displacement (LVDT I - mm).

These results have been averaged in Figure 4. The test series and the number of bulbs along the embedment length (in parenthesis) are indicated. Rupture of the cable always occurred at the barrel and wedge grip. It was observed that the bolt was likely to rupture at any time after the onset of cable yielding, which corresponds to a definite reduction in stiffness above 240-250kN. As expected, for all of the Garford bulb samples, axial loads exceeding the cable capacity were attained.

##### 4.1 Bond Stiffness

Figure 4 indicates that the cable bolt stiffness was almost independent of test parameters for loads less than 70kN. Above this, the rate of load increase, which progressively decreases during a test, was higher for:

- (i) closer bulb spacings\*,
- (ii) longer embedment lengths, and,
- (iii) higher radial stiffness of the confining medium.

These results are summarized in Figure 5, in which the mean (*i.e.* secant) bond stiffness has been plotted against bulb frequency ( $f_b=1/l_b$ ). The mean bond stiffness is the slope of a line joining the origin to that point on the pull curve at which the axial load equals 240kN. *i.e.* it is the secant stiffness over the range 0-240kN.

For bulb frequencies greater than  $3m^{-1}$  (*i.e.* bulb spacings greater than 300mm), the mean bond stiffness is almost independent of the test parameters. This corresponds to tests with two or more bulbs along the embedment length. Approximately 6mm of exit point slip was required to mobilize 240kN; resulting in an average stiffness of 40 kN/mm. This value may represent an upper limit to the attainable mean bond stiffness using Garford bulb cable.

For bulb frequencies less than  $3m^{-1}$  (*i.e.* bulb spacings less than 300mm), the mean stiffness depends on both the embedment length and the radial stiffness of the confining medium. In addition, another factor comes into play, the distance of the first bulb from the exit point. For 900mm bulb spacings the first bulb was located 450mm from the exit point. Based on the axial stiffness of plain strand (approx. 25kN/mm/m)\*\* , up to 4.5mm of stretch may occur along that length of plain strand, adding to the displacement needed to mobilize 240kN, hence decreasing the stiffness.

\*The only exception to this rule was Test series 1. It is proposed that the explanation for this has to do with the very close bulb spacing (200mm) for which there is almost no standard cable between the bulbs.

\*\*For a 1 m length, a tensile load of 25kN of load will produce 1 mm of stretch.

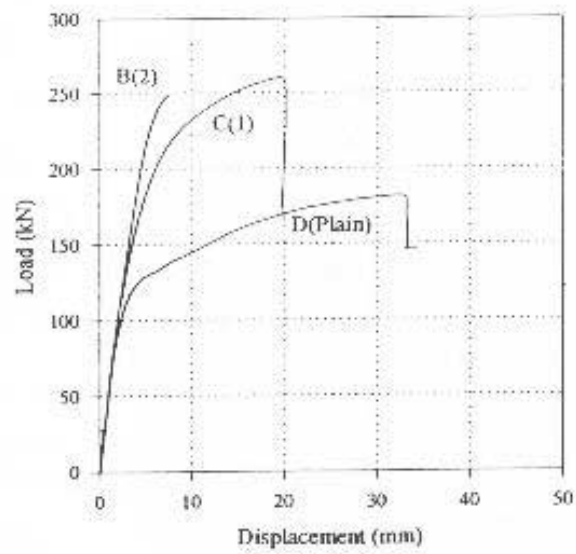
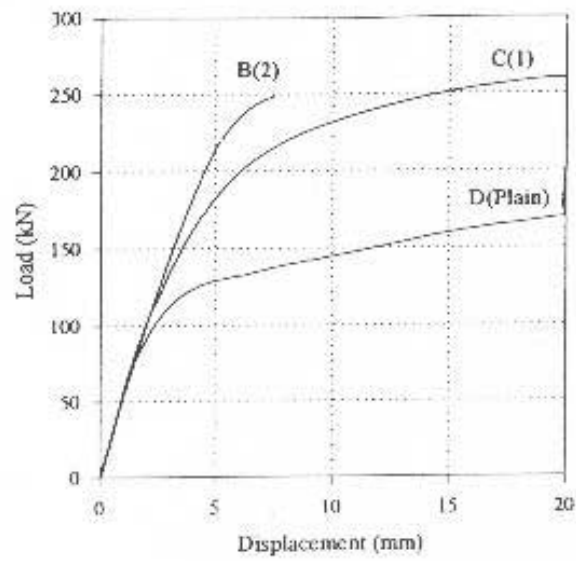


**Figure 4a** Test series B-D, 600mm Embedment length, Aluminum Sch. 80 confinement. The number in parenthesis indicates the number of bulbs along the test section. Test series A which appear to represent an anomalous result have been omitted

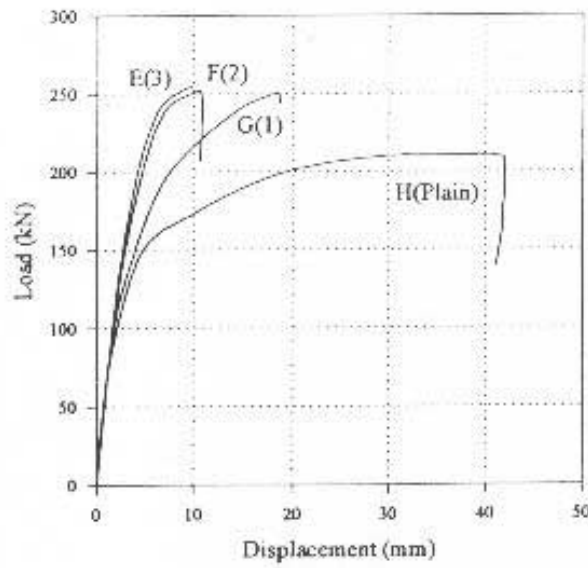
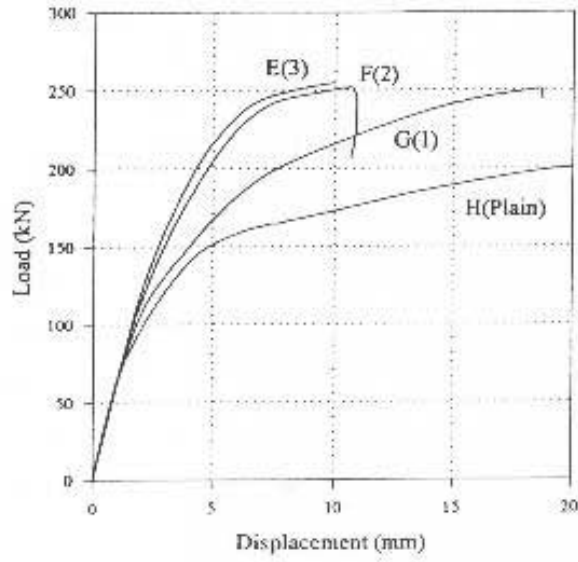


Figure 4b. Test Series E-H. 900mm Embedment length. Sch. 80 Aluminum confinement

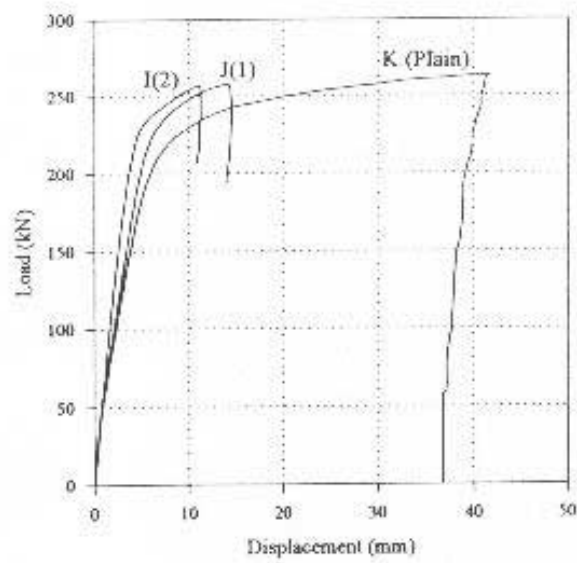
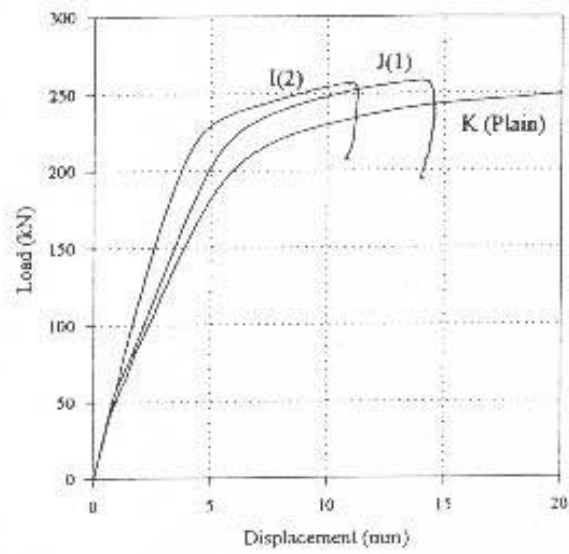


Figure 4c. Test Series I-K. 900mm embedment length. Sch. 80 Steel confinement.

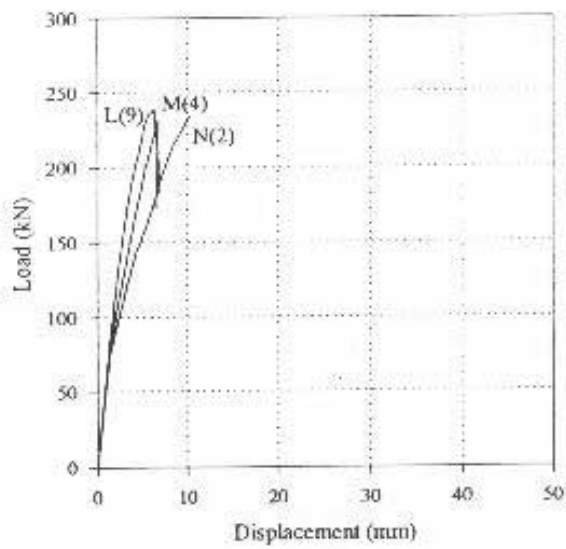
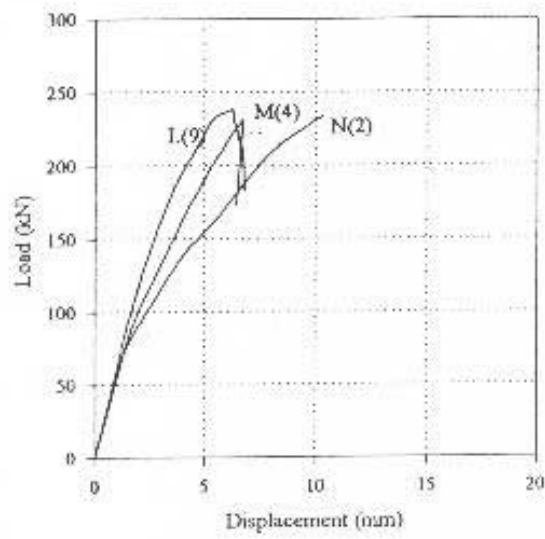


Figure 4d. Test series L-O. 1800mm embedment length. Sch. 80 Aluminum confinement.

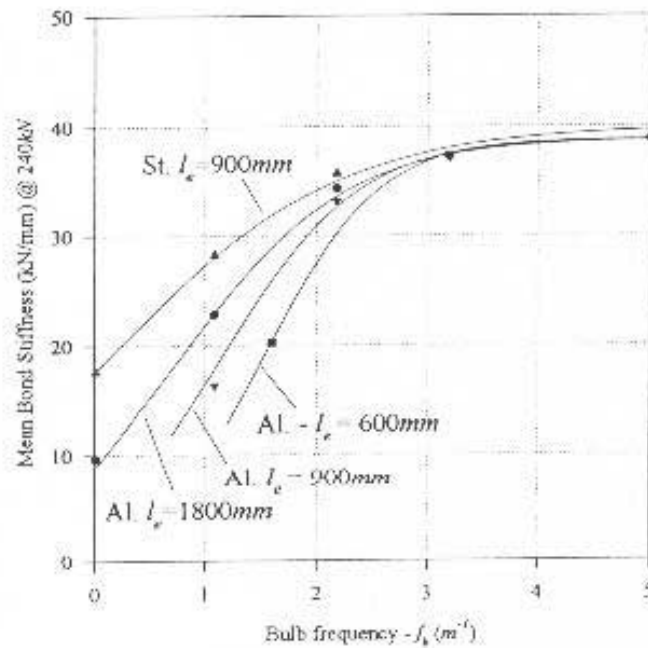


Figure 5: Mean Bond stiffness ( $kN/mm$ ) 0 - 240kN (i.e. 240kN / exit point slip(mm) @ 240kN)

Figure 5 also indicates that the bond stiffness was markedly higher for the test series with a steel pipe. The explanation has to do with the relative proportions of bulb and plain cable along the sample length. Previous research has established that standard cable is more sensitive to confinement than the Garford bulb. For a 300mm bulb spacing plain cable comprises around 50% of the total length; this drops to 33% for the 450mm spacing, and to 17% for 900mm. In other words, for higher bulb spacings the proportion of the cable which is susceptible to the stiffness of the confinement (i.e. the plain cable) increases, and so the cable bolt bond stiffness becomes increasingly sensitive. Although no tests were conducted at different w:c ratio grouts, the same argument will probably apply.

#### 4.2 Transfer length

The concept of *transfer length* ( $l_t$ ) is widely used in civil engineering, especially applications in which pre-tension or post-tension is applied to the strand. Transfer length is defined as : *the length of bond required to transmit the applied tensile load from the member to the grout*. It is the distance along the bonded section at which the tensile stress in the member is less than a specified value (usually 1% of the applied axial load). Farmer(1975) suggests that "the transfer length is equivalent to the optimum design length for the fixed anchorage". As long as the behaviour of both the bolt and the bolt-grout-interface remains elastic the transfer length, as defined above, does not change with the applied axial load. However, for a strand anchorage or bolt, because of the relatively low bond strength, a section of the bond length is likely to debond during stressing and therefore the transfer length will depend on the design load (usually 50-75 % of the ultimate capacity of the member). The results presented above suggest that a higher bulb frequency will decrease the required transfer length. This can potentially reduce the required bond length for end anchored cable bolts which are to be pre-tensioned.

Since, no entry point displacement was detected for samples with two or more bulbs along the embedment length, by definition, for these tests  $l_t$  must be less than the embedment length. Consequently, any further increase in embedment length should not affect the pull test result, because the additional length must not be loaded. Thus, for a 300mm bulb spacing, the response was identical for both a 600mm embedment length and a 900mm embedment length. Although insufficient data exists to accurately determine the critical transfer length for different bulb spacings, as a very general rule of thumb,

$$l_{cts} \cong 2l_b$$

or conservatively

$$l_{cts} < 3l_b$$

where  $l_b$  is the bulb spacing.

This guideline may be used to dimension bond lengths for point anchor bolts.

Note:

It is important to distinguish between critical embedment length ( $l_{ce}$ ) and critical transfer length ( $l_{ct}$ ). *Critical embedment length* is the minimum length of bond necessary to ensure that the ultimate capacity of the bolt is attained. *Critical transfer length* is that length of bond which ensures that when the ultimate capacity of the bolt is reached, no movement of the bolt has occurred at the toe of the bolt. Critical embedment length is always less than critical transfer length. The authors believe that (except for applications involving yielding support) critical transfer length provides a more relevant design parameter for a point anchored bolt, since it ensures that a proportion of the bond length is still relatively intact, and that therefore significant slip at the bolt-grout interface will not occur prior to the ultimate capacity being attained.

#### 4.3 Comparison with a cement grouted rebar.

Four tests were conducted using 25.4mm rebar grouted into a Sch. 80 Aluminum pipe. The cement was identical to that used for the cable pull tests (0.4 w:c ratio, 26-28 day cure). One end of the rebar was threaded and a nut was used to load the bar. Comparing the results shown in Figure 6 with Figure 4b indicates that the load-displacement response of the rebar was not significantly different from that of the Garford bulb with a 300mm bulb spacing. The lower plot shows that for two of the rebar tests some entry point displacement was detected. In other words the transfer length,  $l_t$ , for the rebar is probably slightly longer than for the 300mm spacing Garford bulb cable. Thus, compared to a rebar, the Garford bulb exhibits a similar bond stiffness, and it appears to provide a superior anchor.

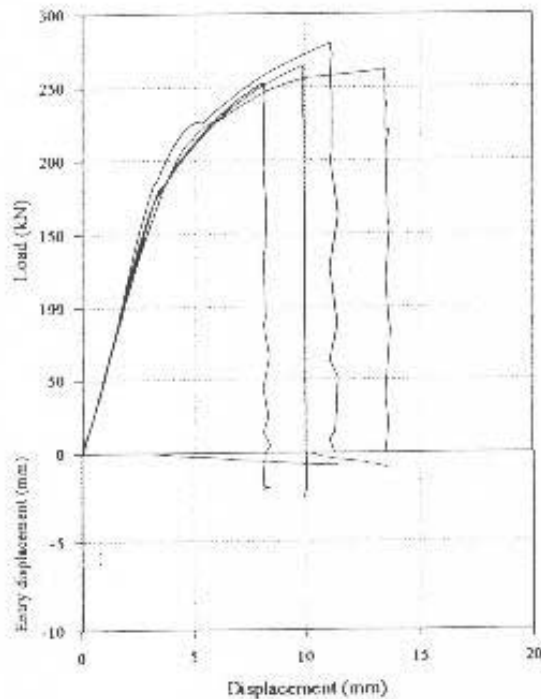


Figure 6: Load versus exit point displacement for a cement grouted 1" rebar.

## 5. Simulation of the pull test results.

### 5.1 Bond Strength and Constitutive model

Within the civil engineering literature tests on both strand and bar are generally conducted at embedment lengths no more than 5 times the bolt diameter. The rationale in using such a short embedment length, is that the shear stress due to bond can be assumed to be constant along the entire test section, and equal to:

$$\tau = \frac{F_p}{l_e \times \pi d_b} \dots \dots \dots (1)$$

where  $d_b$  is the bolt diameter. Furthermore, for short embedment lengths the bond failure process will propagate almost instantaneously.

Following the precedent of Fuller and Cox (1976) the majority of cable bolt tests (Goris, 1990; Hyett *et al.*, 1992; Rajaie, 1990) have been conducted on embedded lengths of 250-300mm, or 15-20 times the diameter. Although propagation of the bond failure process is not instantaneous for these tests, it is reasonable to neglect the associated variation in bond stress along the embedment length. Applying equation (1) to typical pull test results, the relation between bond stress and axial displacement (or slip) can be idealized (Figure 7) as an initial stiff *linear elastic* response prior to what is generally called *bond failure*, though strictly speaking is *bond yield* ( $\tau_y, u_y$ ), followed by a significantly softer though still *work hardening* response until a peak bond strength ( $\tau_p$ ) is reached after significant slip ( $u_p > 20mm$ ). Thereafter, the *residual* response is *perfectly plastic*.

### 5.2 Governing equations for long embedment lengths

For the long pipe tests conducted in this report, the embedment lengths are up to 100 times the bolt diameter. A comparison of the entry point displacement with the exit point displacement indicates that different sections of the cable have slipped by different amounts, so that the bond strength, which varies with slip, must vary significantly along the cable. Furthermore, for such long embedment lengths the bond failure process will gradually propagate from the exit point where load is applied towards the entry point where the cable is free. In order to assess the relation between the mechanics of progressive bond failure and the pull test profiles presented in Section 4 and Appendix A, an analytical model originally developed by Farmer (1975) and Aydan (1989), will be introduced.

The governing equations for the problem describe the force balance along a one dimensional linear elastic member (*i.e.* the bolt) subjected to a combination of axial load and shear stresses that develop due to bond (Figure 8). In Appendix B, the resultant linear differential equation:

$$\frac{d^2 w_b}{dx^2} - \frac{2}{E_b r_b} \tau = \frac{d^2 w_b}{dx^2} - \alpha^2 w_b = 0 \dots \dots \dots (2)$$

where the notation is outlined in Appendix B, is solved for the three stages of the constitutive behaviour (linear elastic, hardening and residual). The resulting simulations predict the relation

between slip, axial force and shear stress along a cable for any specified embedment length. At the exit point and entry point, these can be compared with the experimental results.

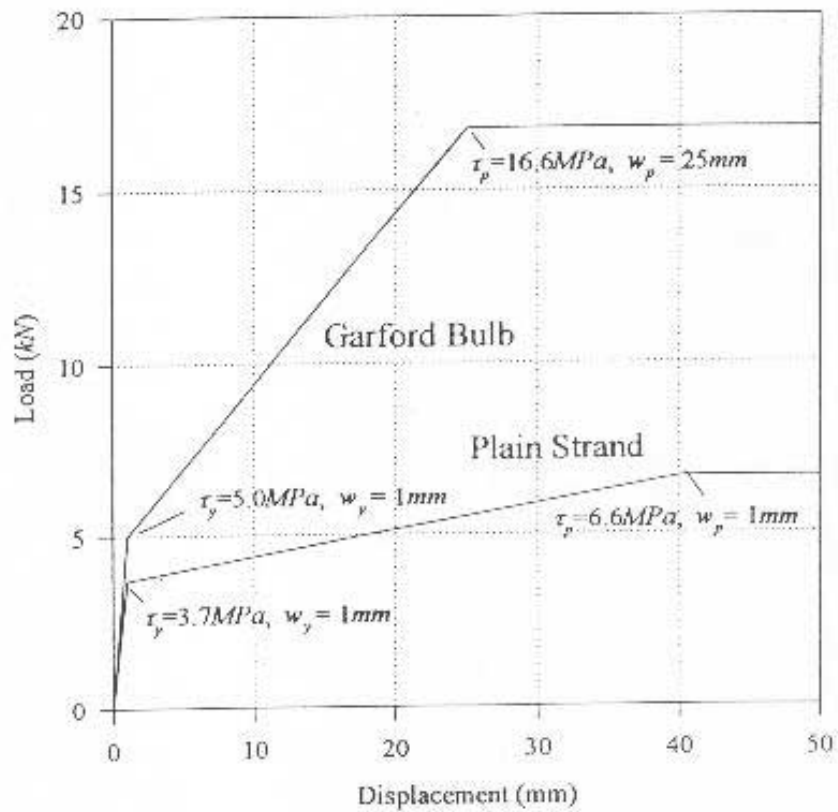


Figure 7. Constitutive model for plain strand and Garford bulb based on short embedment length test: Plain strand - Hyett *et al.*, 1992; Garford bulb cable- Hyett *et al.*, 1995. The values of  $\tau_y$ ,  $w_y$  and  $\tau_p$  and  $w_p$ , that describe an idealized constitutive model are indicated. In the following text, what is strictly *bond yield* will be referred to by the more common term *bond failure*.

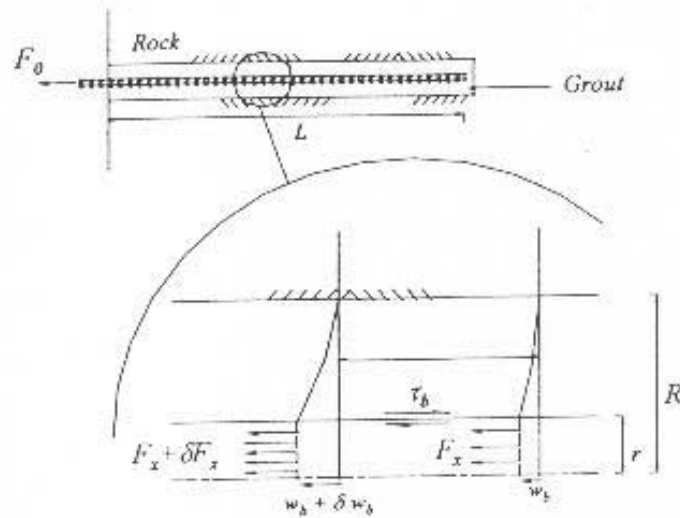
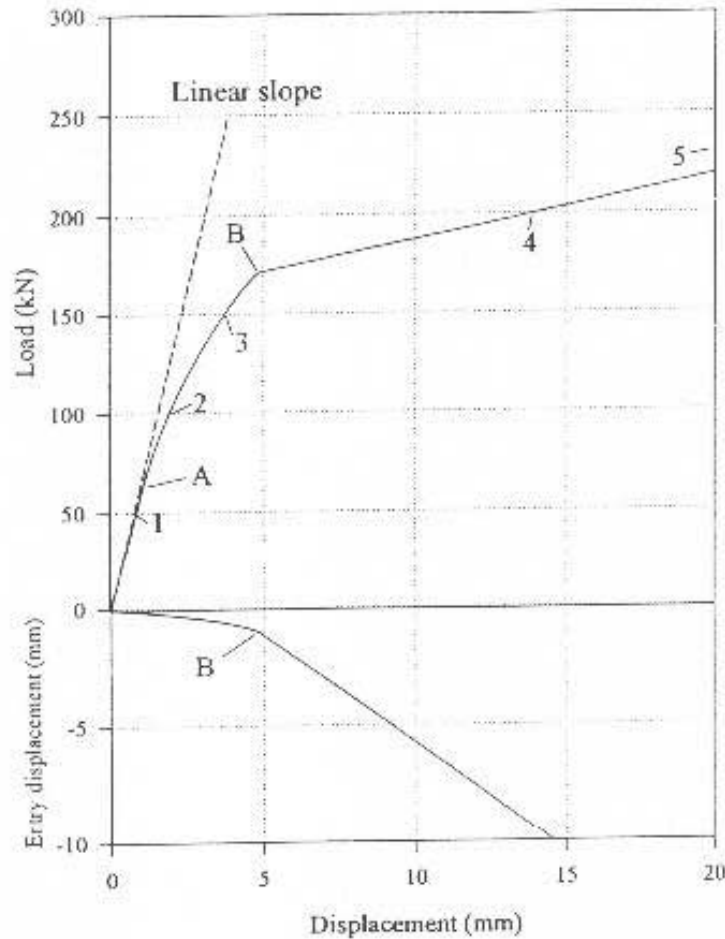


Figure 8. Stress and displacement along a fully grouted bolt

### 5.3 Simulation results for standard cable

Figure 9 shows a simulated pull test for a standard cable embedded in a 900mm long aluminium pipe. Several distinctive features of the simulated pull test profile are evident:

- (i) The departure from non linearity at approximately 60kN (Point A) corresponds to the occurrence of bond failure at the exit point.
- (ii) The subsequent curvilinear profile (A to B) results from the propagation of bond failure along the embedment length.
- (iii) The distinct "elbow" in the load displacement curve and also in the entry point displacement plot (point B), corresponds to the occurrence of bond failure at the entry point so that the entire embedment length has yielded.
- (iv) although not shown in this plot, at approximately 35mm of axial displacement the cable reaches its ultimate capacity. It should be noted that in these simulations no account is taken of the cable yielding prior to rupture. It is a rather trivial matter to implement this in a latter model.



**Figure 9.** Simulated load displacement plot for a 900mm embedment length test in a Sch. 80 Aluminum pipe. Point A, the departure from linearity, corresponds to the onset of bond failure at the entry point. Point B, corresponds to bond yield at the entry point. Between point A and B, bond yield propagates from the exit point to the entry point.

Figure 10 shows the distribution of axial displacement, shear stress due to bond, and axial force along the cable at applied exit point loads of 50kN(1), 100kN(2) etc. The propagation of bond yield is clearly displayed in (c) which shows the distribution of shear stress mobilized at the bolt-grout interface. The reader is urged to take a moment and carefully consider the inter-relations between Figures 11 and 12.

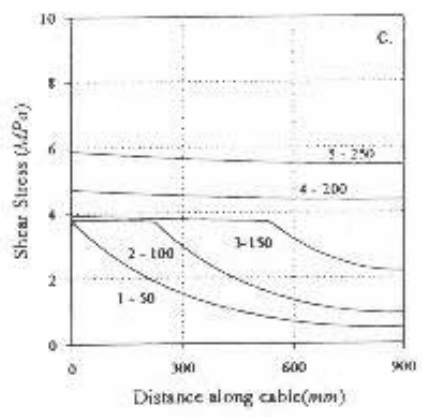
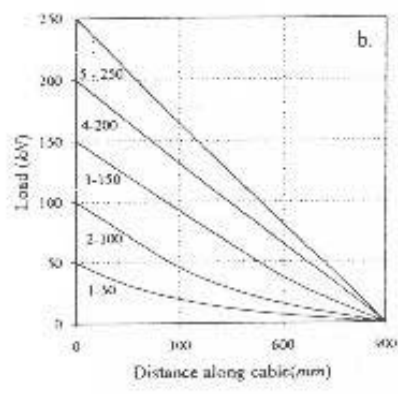
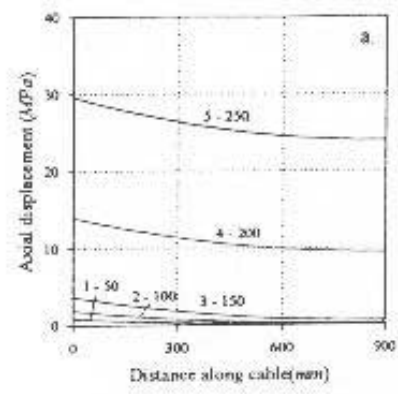


**Figure 10:** Simulations of the distribution of (a) axial displacement or slip, (b) axial force and (c) shear stress due to bond, along a 900mm length of plain cable. Numbers refer to Figure 9.

Figure 11 shows simulations of the effect of embedment length on pull out response for standard cable. For the 250mm embedment length simulation the entry point and exit point displacements are almost the same during the test. This suggests that, as assumed above, the bond stress (which is a function of slip) is probably quite uniform along the test section. As expected the change in slope that occurs due to bond failure along the whole cable increases with embedment length because it takes longer for the bond failure to propagate along the test section to the entry point. For the 1800mm embedment length the cable ruptures before this happens.

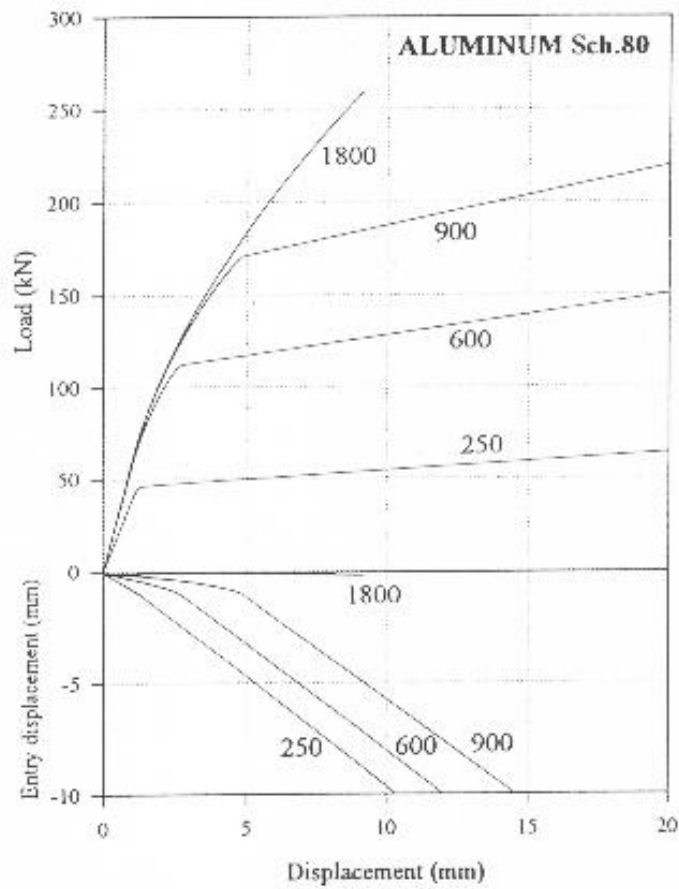
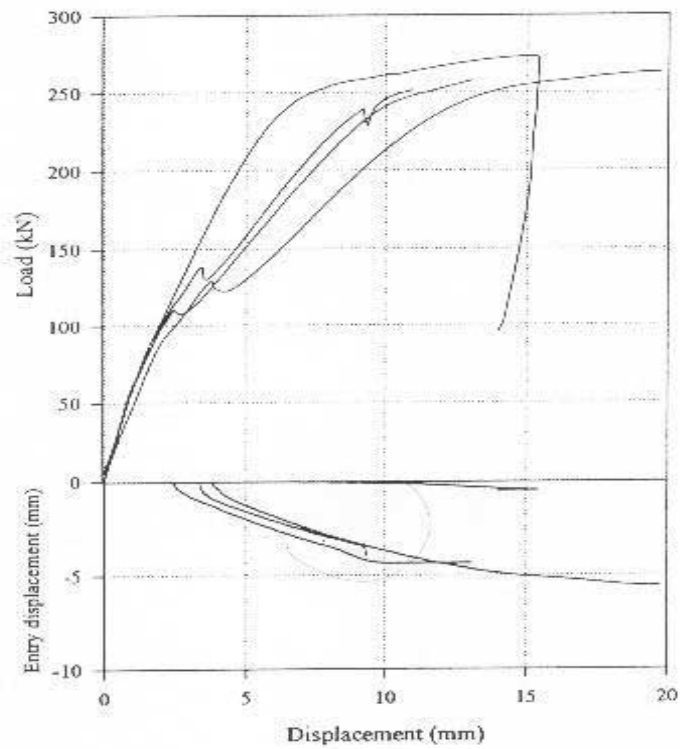


Figure 11. Pull test simulations for plain strand confined by a Sch. 80 aluminum pipe. Numbers represent embedment lengths.

*Appendix A: Individual pull test results.*

### TEST SERIES A

*Embedment Length: 600mm*  
*Bulb Spacing: 200mm*  
*Confining medium: Al.80*

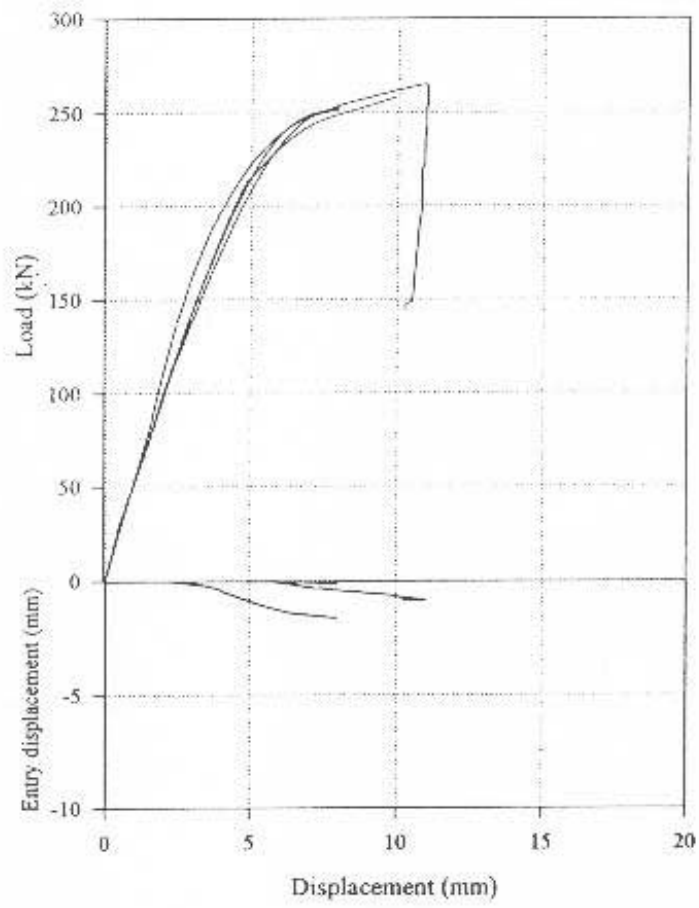


## TEST SERIES B

*Embedment Length: 600mm*

*Bulb Spacing: 300mm*

*Confining medium: Al.80*



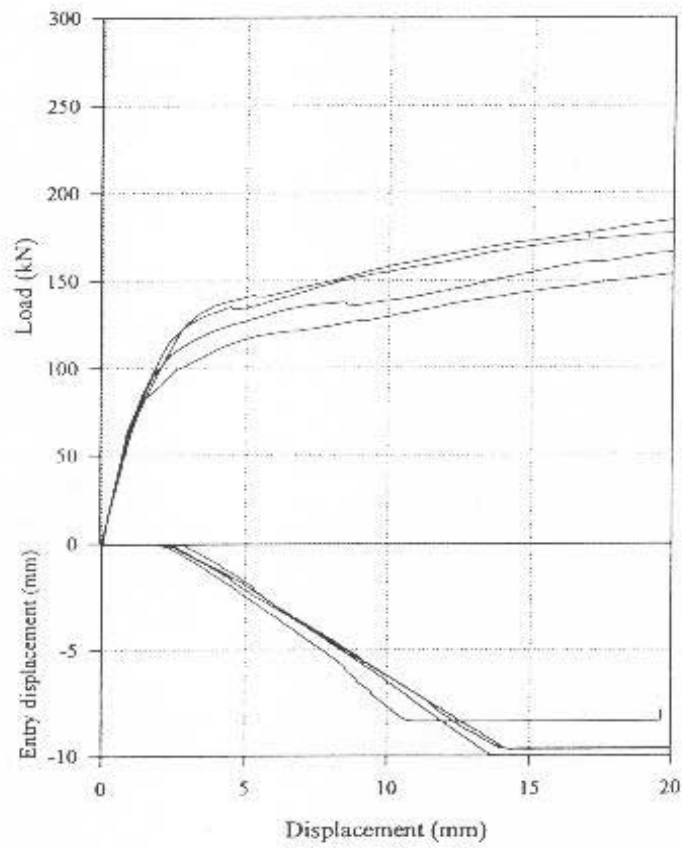


**TEST SERIES D**

*Embedment Length: 600mm*

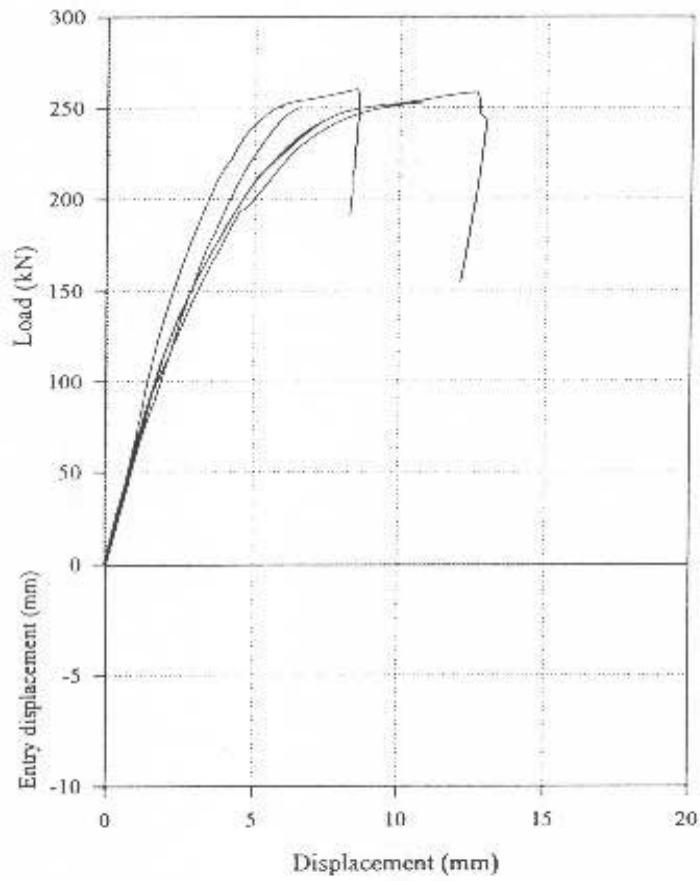
*Bulb Spacing:  $\infty$*

*Confining medium: Al.80*



### TEST SERIES E

*Embedment Length: 900mm*  
*Bulb Spacing: 350mm*  
*Confining medium: Al.80*

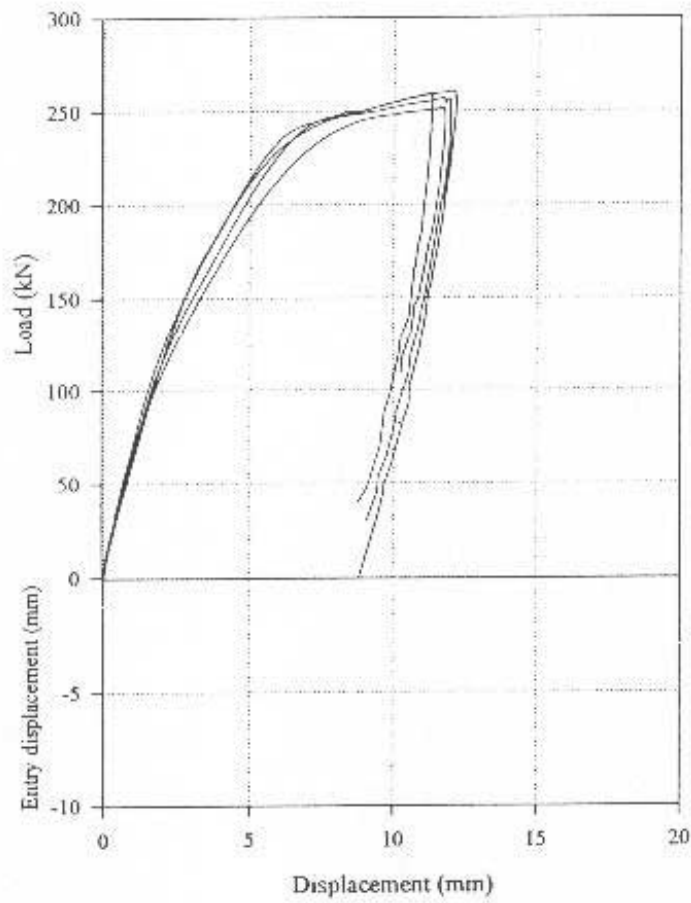


### TEST SERIES F

*Embedment Length: 900mm*

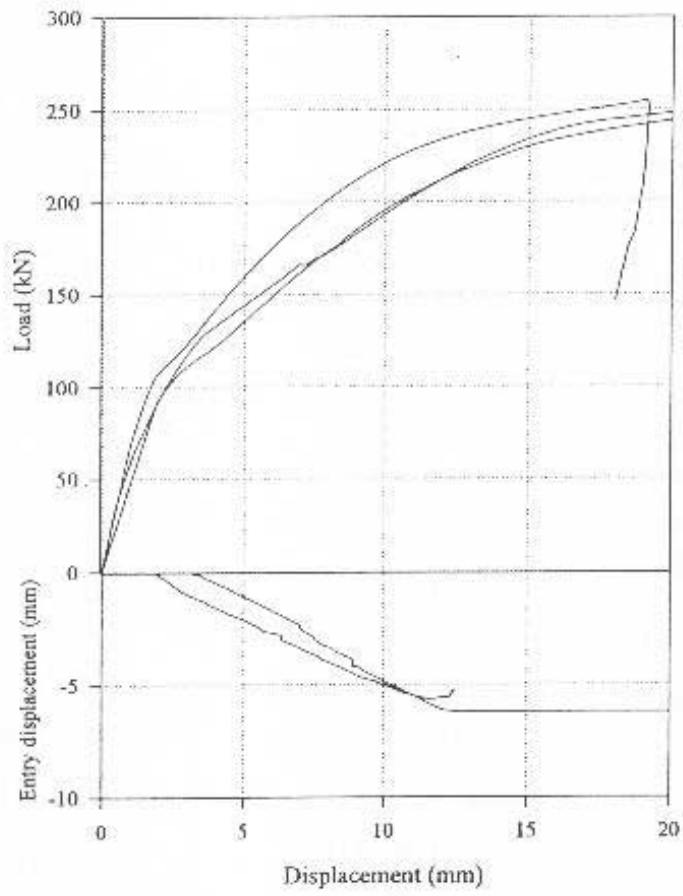
*Bulb Spacing: 450mm*

*Confining medium: Al.80*



### TEST SERIES G

*Embedment Length: 900mm*  
*Bulb Spacing: 900mm*  
*Confining medium: A1.80*

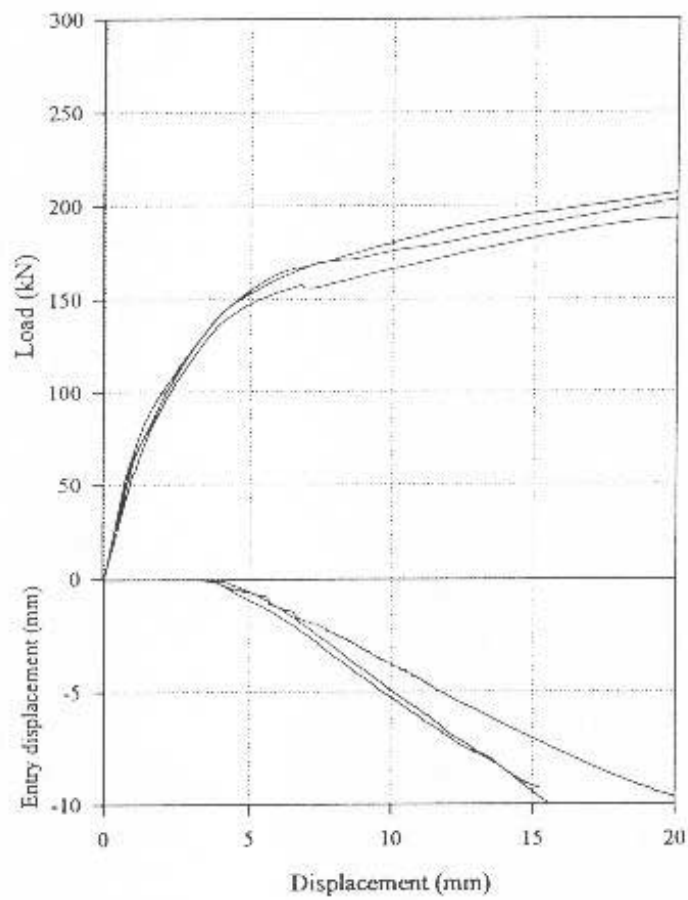


### TEST SERIES H

*Embedment Length: 900mm*

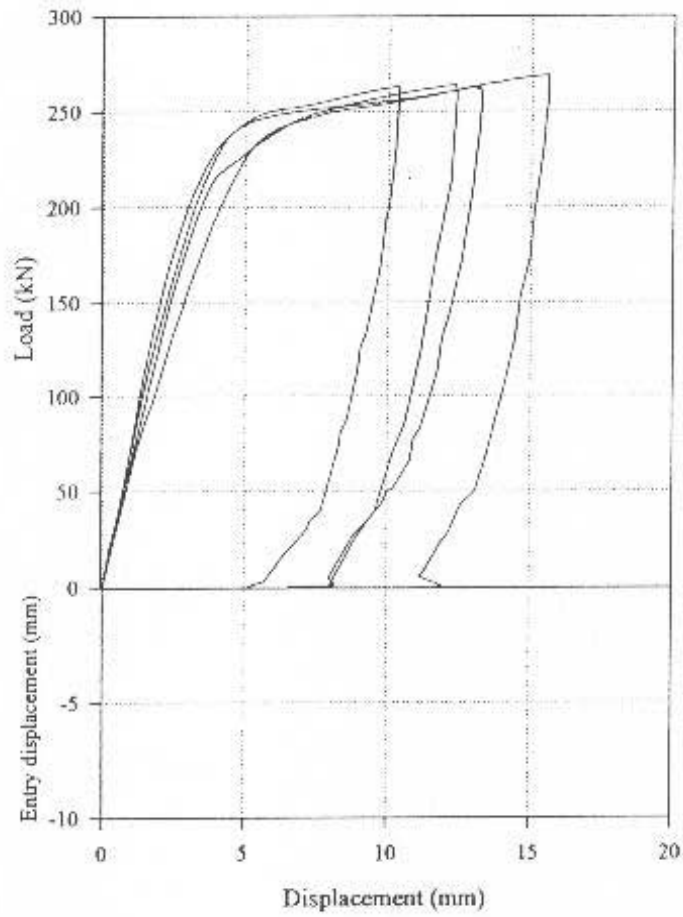
*Bulb Spacing:  $\infty$*

*Confining medium: Al.80*



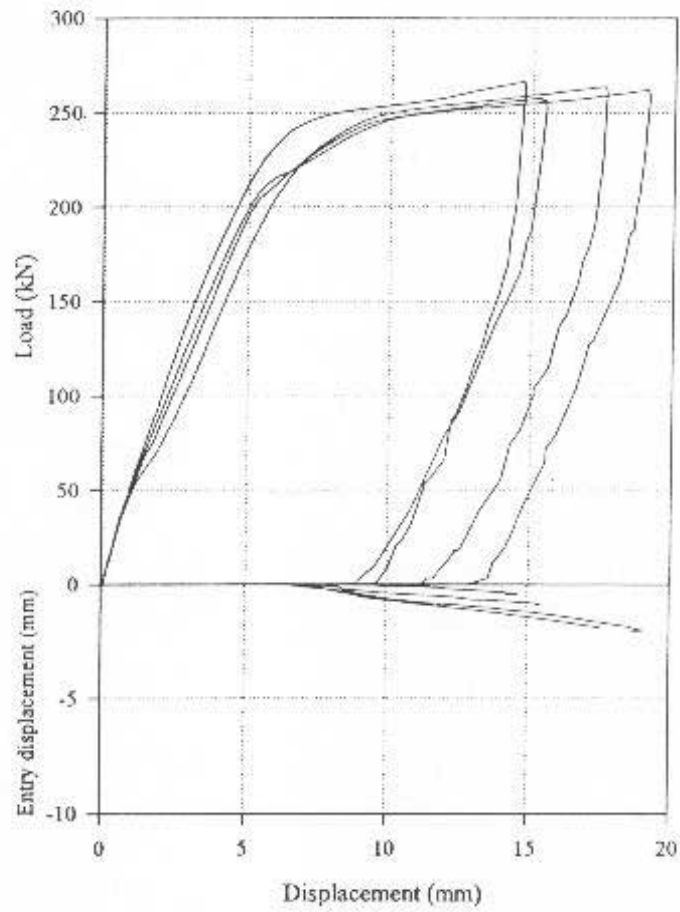
### TEST SERIES I

*Embedment Length: 900mm*  
*Bulb Spacing: 450mm*  
*Confining medium: St.80*



### TEST SERIES J

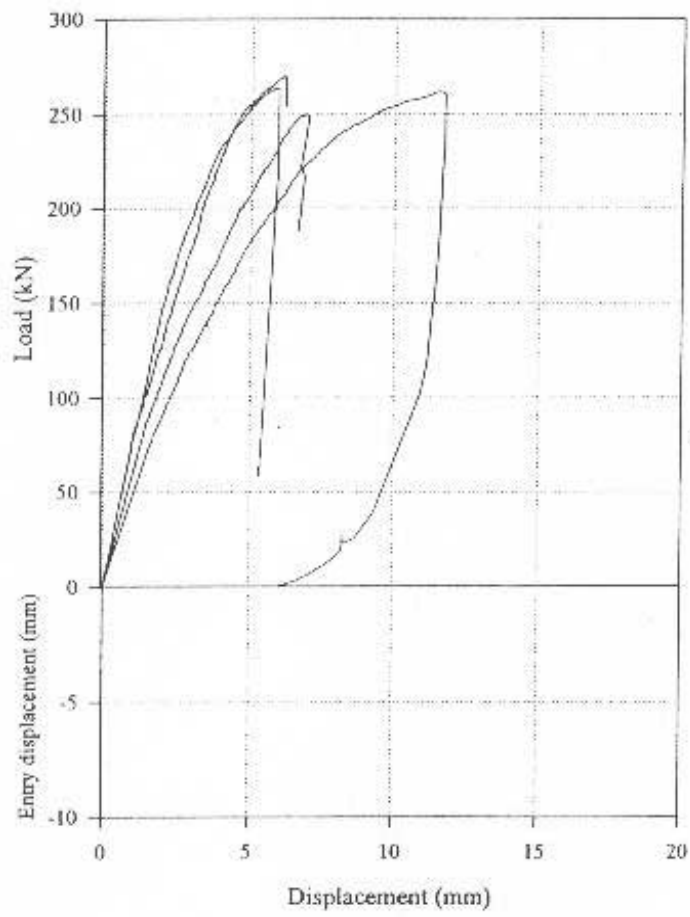
*Embedment Length: 900mm*  
*Bulb Spacing: 450mm*  
*Confining medium: St.80*





### TEST SERIES L

*Embedment Length: 1800mm*  
*Bulb Spacing: 200mm*  
*Confining medium: Al.80*

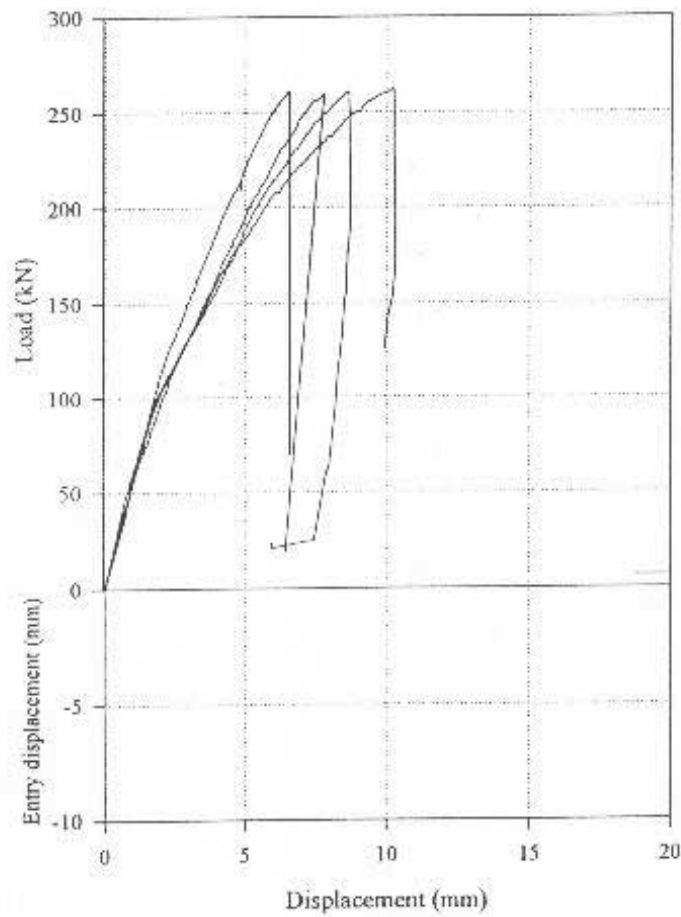


### TEST SERIES M

*Embedment Length: 1800mm*

*Bulb Spacing: 450mm*

*Confining medium: Al.80*

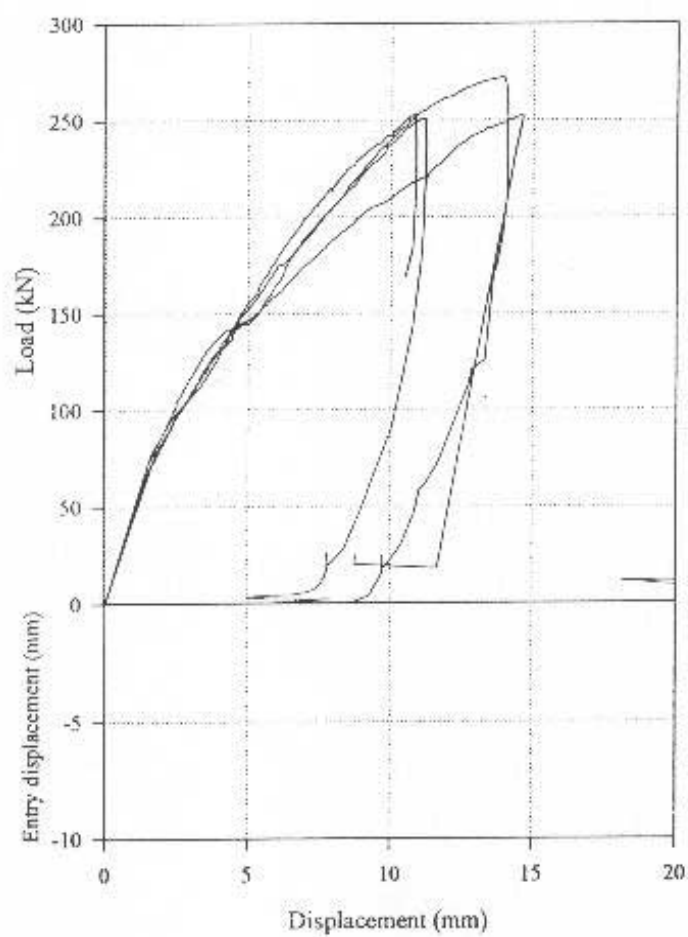


### TEST SERIES N

*Embedment Length: 1800mm*

*Bulb Spacing: 900mm*

*Confining medium: Al.80*



*Appendix B: Analytical Model for the behaviour of fully grouted bolts.*

### B.1 Governing Equations:

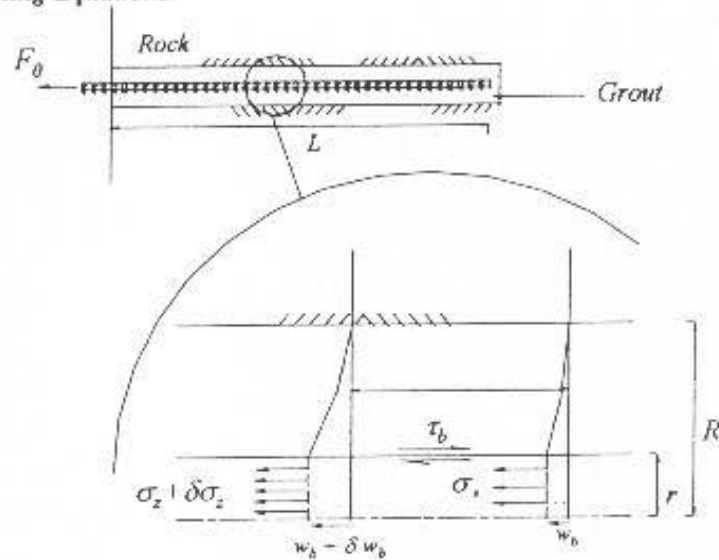


**Figure B1:** Stress and displacement along a grouted bolt.

Following Aydan (1989), consider a bar subjected to an axial load and assume that the bar is one dimensional. The load applied to the bar is assumed to be transferred to the surrounding grout medium as a surfacial shear stress (Figure B1). For a unit slice, the force equilibrium written in terms of stresses gives:

$$\frac{d\sigma_z}{dz} + \frac{2}{r_b} \tau = 0 \quad (\text{B1})$$

where  $\sigma_z$  is the axial stress in the bar,  $\tau$  is the shear stress due to bond acting on the outer surface of the bar, and  $r_b$  is the radius of the bar.

### B.2 Constitutive behaviour for bond.

The constitutive behaviour for bond describes the relation between bond strength (the axial load divided by the surface area of the bar or strand) and axial displacement of the bar. We will assume that this is divisible into three stages: (i) linear elastic (ii) work hardening and (iii) residual (Figure B1). Yield of the interface occur when:

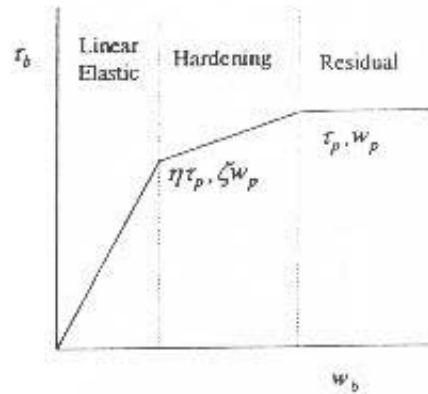


Figure B2: Constitutive behaviour for the bolt grout interface.

Considering the general case when the load is increased at one end of the bar with the other end free. In the initial stages the bond will be elastic along the whole length (CASE 1) of the bolt. As the applied axial force continues to increase the interface will yield ( $L_1 > 0$ ), first at  $z = 0$  where the load is applied, and thereafter progressively along the bolt length. Eventually as the load continues to increase peak bond strength will be reached at  $z = 0$  and residual behaviour will propagate along the bolt length (CASE 2). Depending on the bolt length, the bond will yield and even reach peak at the unloaded end  $z = l$ .

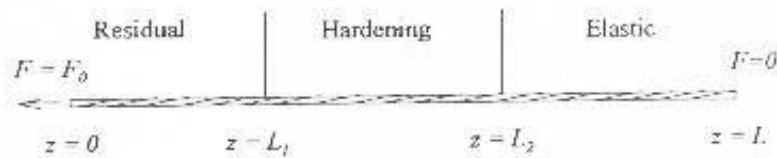


Figure B2: Distribution of constitutive behaviour of a long bolt

### B.3 CASE 1: Solution for Linear Elastic interface behaviour along whole bolt length.

This solution was originally presented by Farmer (1975) and later by Aydan (1989).

From Figure B2, the elastic relation between bond stress and axial displacement (*i.e.* the initial stiffness) at the bolt-grout interface is:

$$\tau_b = \frac{\eta r_p}{\xi w_p} w_b \quad (\text{B2})$$

Substituting into equation B1 gives,

$$\frac{d^2 w_b}{dz^2} - \alpha^2 w_b = 0 \quad (\text{B3})$$

where,

$$\alpha = \sqrt{\frac{2 \eta r_p}{E_b r_b \xi w_p}} \quad (\text{B4})$$

The solution to equation B3 is:

$$w_b = A_1 e^{\alpha z} + A_2 e^{-\alpha z} \quad (\text{B5})$$

The integration constants  $A_1$  and  $A_2$  can be found from the boundary conditions:  $\sigma_z = \sigma_0$  at  $z=0$  and  $\sigma_z = 0$  at  $z=L$ ,  $L$  being the length of the bolt. They are:

$$A_1 = \frac{\sigma_0}{E_b \alpha} \frac{e^{-\alpha L}}{e^{\alpha L} - e^{-\alpha L}}, \quad A_2 = \frac{\sigma_0}{E_b \alpha} \frac{e^{\alpha L}}{e^{\alpha L} - e^{-\alpha L}} \quad (\text{B6})$$

and accordingly:

$$w_b = \frac{\sigma_0}{E_b \alpha} \frac{e^{\alpha(L-z)} + e^{-\alpha(L-z)}}{e^{\alpha L} - e^{-\alpha L}}, \quad (\text{B7})$$

the axial stress in the bolt is:

$$\sigma_z = \sigma_0 \frac{e^{\alpha(L-z)} - e^{-\alpha(L-z)}}{e^{\alpha L} - e^{-\alpha L}}, \quad (\text{B8})$$

and the shear stress at the bolt grout interface is:

$$\tau_b = \frac{\sigma_g r_b \alpha}{2} \frac{e^{\alpha(L-z)} - e^{-\alpha(L-z)}}{e^{\alpha z} - e^{-\alpha z}} \quad (\text{B9})$$

### Solution for Elastic, Hardening and Residual Grout-Bolt Interface Behaviour.

The general case is shown in Figure B3,

#### Section with Residual Behaviour of the Grout-Bolt Interface ( $0 < z < L_1$ )

The shear strength due to bond along this section of the bolt is  $\tau_b = \tau_p$ . Thus, from Equation B1 :

$$\frac{d^2 w_b}{dz^2} - \frac{2\tau_p}{E_b r_b} = 0 \quad (\text{B10})$$

which has the general solution:

$$w_b = \frac{2\tau_p}{E_b r_b} \frac{z^2}{2} + C_1 z + C_2 \quad (\text{B11})$$

Using the boundary conditions:  $w_b = w_p$  at  $z = L_1$  and  $\sigma_z = \sigma_0$  at  $z = 0$ , B11 becomes

$$w_b = w_p + \frac{\tau_p}{E_b r_b} (z^2 - L_1^2) - \frac{\sigma_0}{E_b} (z - L_1) \quad (\text{B12})$$

and

$$\sigma_z = \sigma_0 - 2 \frac{\tau_p}{r_b} z \quad (\text{A12})$$

#### Section with work hardening behaviour for the bolt-grout interface ( $L_1 < z < L_2$ )

The shear strength due to bond along this section of the bolt is  $\tau_b = \tau_p$

$$\tau_b = \frac{\tau_p}{w_p} \frac{(1-\eta)}{(1-\xi)} w_b + \tau_p \frac{\eta - \xi}{1-\xi} \quad (\text{B13})$$

Hence, from equation B1 the differential equation to be solved is:

$$\frac{d^2 w_b}{dz^2} - \frac{2}{E_b r_b} \frac{\tau_p (1-\eta)}{w_p (1-\xi)} w_b = \frac{2}{E_b r_b} \tau_p \frac{\eta - \xi}{1-\xi} \quad (\text{B14})$$

The solution for  $w_b$  is:

$$w_b = B_1 e^{\beta z} + B_2 e^{-\beta z} - w_p \frac{\eta - \xi}{1-\eta} \quad (\text{B15})$$

where:

$$\beta = \sqrt{\frac{2\tau_p (1-\eta)}{E_b r_b w_p (1-\xi)}} \quad (\text{B16})$$

Introducing the boundary conditions:  $\tau_b = \tau_p$  at  $z=L_1$ , and  $\tau_b = \eta\tau_p$  at  $z=L_2$ ,

$$B_1 = \frac{2\tau_p}{E_b r_b \alpha^2} \frac{\eta e^{-\alpha L_1} - e^{-\alpha L_2}}{e^{\alpha(L_2-L_1)} + e^{-\alpha(L_2-L_1)}} \quad B_2 = \frac{2\tau_p}{E_b r_b \alpha^2} \frac{\eta e^{\alpha L_1} - e^{-\alpha L_2}}{e^{\alpha(L_2-L_1)} + e^{-\alpha(L_2-L_1)}} \quad (\text{B17})$$

It follows that

$$\sigma_z = \beta B_1 e^{\beta z} - \beta B_2 e^{-\beta z}, \quad (\text{B18})$$

$$\tau_b = \beta^2 B_1 e^{\beta z} + \beta^2 B_2 e^{-\beta z} \quad (\text{B19})$$

#### *Section with Elastic Behaviour of the Grout-Bolt Interface ( $L_2 < z < L$ )*

The solution to this problem is given by equation A5. Using the boundary conditions

The integration constants  $A_1$  and  $A_2$  can be found from the boundary conditions:

$\tau_b = \eta\tau_p$  at  $z=L_2$  and  $\sigma_z = 0$  at  $z=L$ ,  $L$  being the length of the bolt. They are:

$$A_1 = \frac{2\eta\tau_p}{E_b r_b \alpha^2} \frac{e^{-\alpha L}}{(e^{-\alpha(L-L_2)} - e^{\alpha(L-L_2)})}, \quad A_2 = \frac{2\eta\tau_p}{E_b r_b \alpha^2} \frac{e^{\alpha L}}{(e^{-\alpha(L-L_2)} - e^{\alpha(L-L_2)})} \quad (\text{B20})$$

and accordingly:

$$w_b = \frac{2\eta\tau_p}{E_b r_b \alpha^2} \frac{e^{-\alpha(L-z)} + e^{\alpha(L-z)}}{(e^{-\alpha(L-L_2)} - e^{\alpha(L-L_2)})}, \quad (\text{B21})$$

the axial stress in the bolt is:

$$\sigma_z = \frac{2\eta\tau_p}{r_b \alpha} \frac{e^{-\alpha(L-z)} - e^{\alpha(L-z)}}{(e^{-\alpha(L-L_2)} - e^{\alpha(L-L_2)})} \quad (\text{B22})$$

and the shear stress at the bolt grout interface is:

$$\tau_b = \eta\tau_p \frac{e^{-\alpha(L-z)} + e^{\alpha(L-z)}}{(e^{-\alpha(L-L_2)} - e^{\alpha(L-L_2)})} \quad (\text{B23})$$

Using the relations for bolt displacement ( $w_b$ ) and axial stress ( $\sigma_z$ ) and the conditions for continuity and equilibrium between the elastic, hardening and residual zones,  $L_1$  and  $L_2$  can be found and hence the distribution of  $w_b$ ,  $\sigma_z$  and  $\tau_b$  along the bolt. Examples are given in the text.

#### 5.4 Simulation results for Garford bulb cable

To conduct similar simulations on the Garford bulb cable, the constitutive parameters given in Figure 9 were used. Since, these are based on a  $300\text{mm}$  embedment length with a single bulb located at the midpoint, the simulations correspond to a  $300\text{mm}$  bulb spacing. Figure 12 is a simulation for a  $900\text{mm}$  embedment length pull test confined in an aluminum pipe. Figure 13 shows the distribution of axial displacement, axial force and shear stress along the cable as axial load is progressively applied to the cable. The propagation of the bond failure process is particularly well shown in (c). At  $50\text{kN}$  (lowest profile) the bond is still intact, and as the axial load is increased the point at which the bond fails migrates towards the entry point. In contrast to the plain cable result, when the cable ruptures at  $250\text{kN}$  the bond has still not failed along the whole embedment length.

Figure 14 shows the results of simulated tests for different embedment lengths. Notice that:

- the effects of increasing the embedment length from  $900\text{mm}$  to  $1800\text{mm}$  are negligible;
- the requirement for at least  $5\text{mm}$  of exit point displacement to mobilise the capacity of the cable appears to be confirmed by the simulation;
- for tests at  $900\text{mm}$  and  $1800\text{mm}$  the bond does not fail along the whole cable bolt length, and for these tests very little entry point displacement is predicted.

In summary, for both the standard cable and the Garford bulb cable, the simulated load displacement response have a strong qualitative and quantitative resemblance to the experimental pull test results. For example, in Figure 11 the  $900\text{mm}$  embedment length results correspond to test series H. The majority of the characteristics including the departure from non linearity at  $60\text{kN}$ , the curvilinear response between 1 and  $5\text{mm}$ , the onset of significant entry point displacement around  $4\text{-}5\text{mm}$  all agree. Perhaps the most significant discrepancy is that the simulation predicts some entry point displacement prior to  $4\text{mm}$  whereas in practice none is observed. Indeed, this discrepancy exists for all of the simulation results. At present no explanation can be offered for this. However, by significantly dropping the modulus of the cable it is possible to obtain agreement with the pull test results though it is difficult to justify such a change in the input parameters.

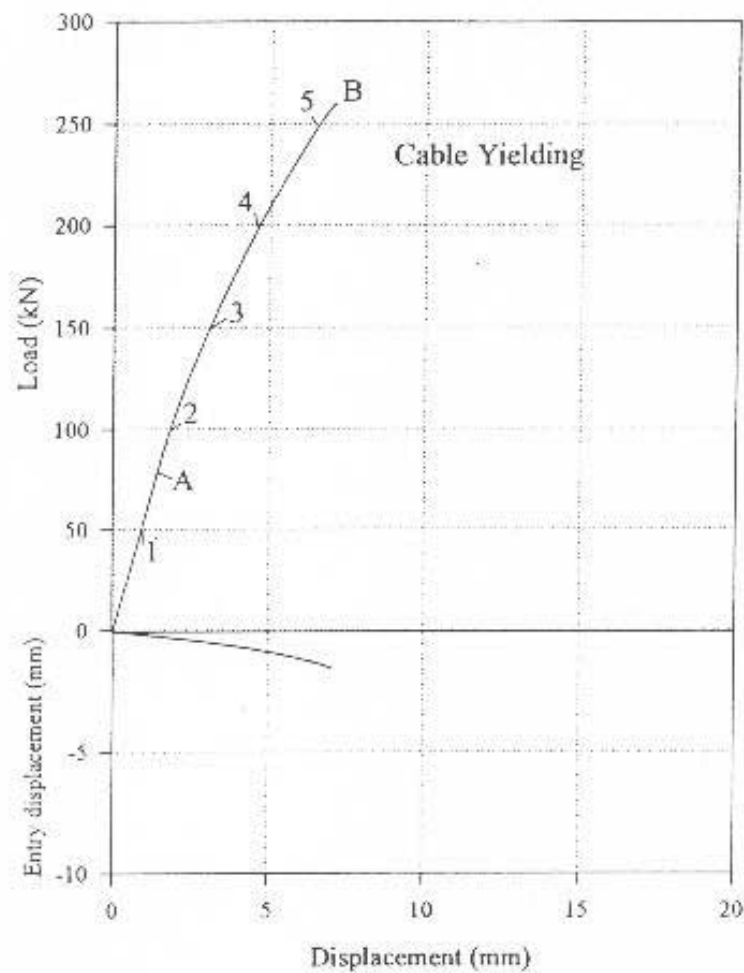


Figure 12. Simulated load displacement plot for a 300mm bulb spacing, in a 900mm embedment length test confined by an Sch. 80 aluminum pipe. Point A, the departure from linearity, corresponds to the onset of bond failure at the entry point. Point B, corresponds to cable rupture. Between point A and B, bond yield propagates from the exit point towards the entry point. The dashed line shows the predicted response if cable yielding were incorporated into the model.

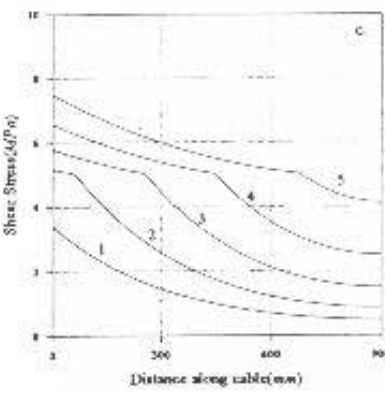
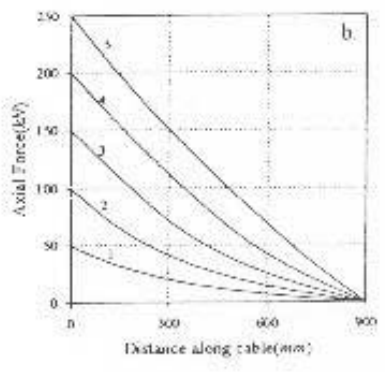
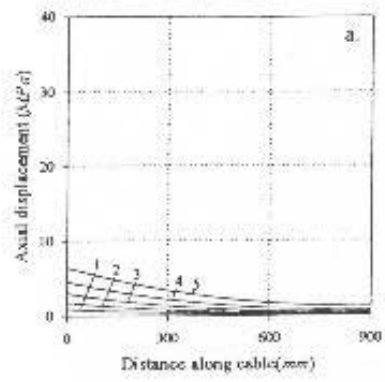


Figure 13: Simulation of the distribution of (a) axial displacement or slip, (b) axial force and (c) shear stress due to bond along a 900mm Garford bulb with 300mm bulb spacing. The numbers refer to points on Figure 12.

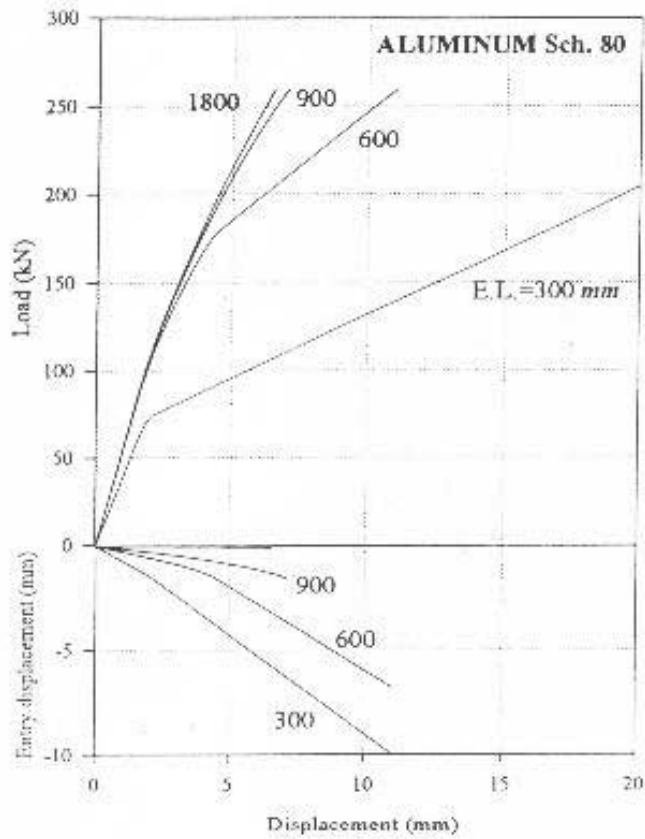


Figure 14. Pull test simulations for 300mm Garford bulb spacing confined by a Sch. 80 aluminum pipe. Numbers represent embedment lengths.

## 6. Implications and Conclusions

The results for 75 pull tests demonstrate the increased bond strength and bond stiffness of fully grouted Garford bulb cable compared to plain strand. Furthermore, the stiffness of fully grouted garford bulb cable can be controlled by varying the bulb frequency.

The test results indicate that for loads less than  $60kN$ , the bond stiffness was relatively independent of test parameters. However, at higher loads, the rate of load increase during a cable pull test (*i.e.* the stiffness of the grouted cable bolt) was higher for:

- (i) closer bulb spacings (except Test Series A)\* ,
- (ii) longer embedment lengths, and,
- (iii) higher radial stiffness of the confining medium.

For bulb frequencies greater than  $3m^{-1}$  (*i.e.* bulb spacings greater than approx. 12"), the amount of slip required to mobilize  $240kM$  was the same for all the test series. This corresponds to tests with two or more bulbs along the embedment length. In these cases about  $6mm$  of exit point displacement was required regardless of the test parameters. This suggests that the bulb requires some relative slip with the cement in order to mobilize bond strength. Furthermore, it implies there is an upper limit to the bond stiffness of a Garford bulb cable bolt.

For bulb frequencies less than  $3m^{-1}$  (*i.e.* bulb spacings less than approx. 12"), the stiffness depends primarily on both the embedment length and the radial stiffness of the confining medium.

No slip was detected at the entry point for samples with two or more bulbs along the embedment length. This result corresponds to the observation that the stiffness did not increase significantly for samples with more than two bulbs along the embedment length, since the additional bulbs must not be loaded.

These observations agree well with analytical simulations that model the propagation of bond failure along any length of fully grouted cable. This establishes that, using input data from short embedment length tests, it is possible to predict the behavior of long embedment lengths, such as those used in both civil engineering and mining engineering practice.

\*For Test Series A, the very close proximity of the bulbs, resulting in almost no standard cable between them may result in unreliable performance.

## 7. References

- Aydan, O., (1989), *The stabilization of engineering structures by rockbolts*, DEng. thesis, Nagoya University, Japan.
- Farmer, I. W., (1975), "Stress distribution along a resin grouted anchor", *Int. J. of Rock Mech. and Min. Sci. Geomech. Abstr.* Vol 12, pp 347-351.  
*Tunnels & Tunneling*, Vol 10, pp 37-40.
- Fuller, P.G. and Cox, R.H.T., (1975), "Mechanics of load transfer from steel tendons to cement based grouts", *Proc. 5th Aust. Conf. on the Mechanics of Structures and Materials*, Melbourne, Australia, pp 189-203.
- Garford Pty. Ltd, (1990). "Garford bulb anchor, Ground support", 3 page catalogue.
- Goris J.M, (1990). " Laboratory evaluation of cable bolt supports", 92nd annual general meeting of CIM.
- Hyett, A.J., Bawden, W.F. and Reichert, R.D., (1992). " The effect of rock mass confinement on the bond strength of fully grouted cable bolts", *Int. J. of Rock Mechanics & Geomechanical Abstracts*, Vol 29, No. 5, pp 503-524.
- Hyett A.J., Bawden W.F., Hedrick N. and Blackall J., (1995a), "A laboratory evaluation of the 25 mm Garford bulb anchor for cable bolt reinforcement", *CIM magazine*, Vol. 88 No. 992, pp 54-59.

Kaiser, P.K , Yazici, S. and Nose, J., (1992). " Effect of stress change on the bond strength of fully grouted cables", *Int. J. of Rock Mechanics & Geomechanical Abstracts*, Vol 29, No.3 pp 293-306.

Rajaie, H., (1990), "Experimental and numerical investigations of cable bolt support systems", Ph.D thesis, McGill University, Montreal, Canada.

Stillborg B, (1984). " Experimental investigation of steel cables for rock reinforcement in hard rock", *Doctoral thesis, Lulea university, Sweden.*